Verification of Parallel Connected Multiple Motor Drive System with Numbers of Permanent Magnet Synchronous Motors

Tsuyoshi Nagano[1] and Goh Teck Chiang[1] and Jun-ichi Itoh[1] and Koji Kato[2]

[1]Nagaoka University of Technology
1603-1 Kamitomioka-machi
Nagaoka city, Niigata, Japan
Tel.: [1]+81 / (258) – 47.9533.
E-Mail: [1]itoh@vos.nagaokaut.ac.jp
URL: [1]http://itohserver01.nagaokaut.ac.jp/itohlab/en/index.html

[2]Sanken Electric Co., Ltd.
3-6-3 Kitano
Niiza city, Saitama, Japan
[2]+81 / (48) – 472.1111.
[2]k.kato@sanken-ele.co.jp
[2]http:// http://www.sanken-ele.co.jp/en/index.php

Acknowledgements

Keywords

«Permanent magnet motor», «Parallel operation», «Vector control», «AC machine».

Abstract

This paper discusses a multi-parallel drive system for permanent magnet synchronous motors PMSMs). This system proposes to use two different functions of inverter, a main inverter with V/f control to control the speed of all parallel connected PMSMs. Then, each of PMSM is individually connected with an auxiliary inverter. The auxiliary windings which are used in the auxiliary inverter are placed in the slots together with the conventional windings. In addition, implementation of the damping control in the auxiliary inverter is discussed and the stability analysis is evaluated in order to suppress the speed and torque vibrations which are caused from the resonance between the inertia moment and the synchronous reactance. The simulation and experimental results demonstrate the effectiveness of the proposed system. Moreover, the relationship between the damping gain and the output power of the auxiliary inverter is clarified. From the results, it can be confirmed that if the application that is required a slow response is applied in the auxiliary inverter, then the power capacity of the auxiliary inverter can achieve the smallest which is equivalent to 10% of the main inverter power capacity.

1. Introduction

Recently, driving multiple motors in parallel at a time shows a good degree of interests in community. One of the techniques to drive multiple motors in parallel is to employ one large power capacity inverter. One of the advantages of parallel motor drive by one large power capacity inverter is to be able to reduce the numbers of the inverter and system cost. This application is commonly found in the induction motor [1-2]. However, in the case of PMSMs, since each pole position of the PMSM is different to each other, the motor current cannot be controlled to match the rotational coordinates by using only one inverter. Therefore, it is difficult to drive the parallel connected PMSMs by using only one inverter, due to the occurrence of the each phase differences between the rotational coordinates of the inverter and the PMSM. In that case, the torque vibration occurs due to the resonance between a synchronous reactance and the inertia moment of the motor. Therefore, the torque vibration needs to be suppressed in order to drive the PMSMs in parallel.

Numerous studies have shown a number of ways to drive two PMSMs at a time, including the implementation of a five-leg inverter [3-4] and also the implementation of a nine switches inverter [5-6] and so on [7-9]. However, the numbers of parallel units are limited by the number of legs in the

inverter. Especially, it is not practical to drive several ten units of PMSMs by one large capacity inverter at the same time.

The V/f control is suitable for multi-parallel drive for PMSM because the controller does not require the information of the rotor position in the PMSM. The method that PMSM can drive by using the information of the current vibration is also studied [10]. However, this method cannot be applied to the multi-parallel drive system since the vibration of one motor can only be suppressed by one inverter.

In this paper, in order to drive PMSMs in parallel effectively, a multi-parallel drive system of PMSMs based on V/f control is proposed. In the proposed methods, the vibration is suppressed by using the auxiliary inverter. In addition, each of the PMSM is added with auxiliary windings. The method that the iron core of the motor is used for integrating the transformer by using the auxiliary winding is studied [11]. On the other hands, the auxiliary windings, which are connected to a small power capacity inverter, can suppress the torque vibration. The power capacity of the auxiliary inverter is much smaller than that of the main inverter because the power capacity of the auxiliary windings is required to suppress the vibration. Note that the proposed system assumes that the each of the motor in the multi-parallel connected PMSMs is driving at same speed and same load such as fans. Different speed drive systems such as the electric train and electric vehicles are not considered in this paper because the motor speed in each motor is different to each other.

This paper is organized as follows; first, the configuration of the proposed parallel drive system is introduced. Next, the control method of the main inverter with V/f control and the auxiliary inverter with field-oriented control is described. Next, the simulation and experimental results demonstrate that the proposed system can drive multiple of parallel connected PMSMs effectively by suppressing the torque vibration. Then, the stability of the proposed system is analyzed and discussed by using the root locus. Finally, the relationships among the response of the damping control, the overshoot of the motor speed and the power capacity of the auxiliary inverter are clarified.

2. Proposed system and control structure

Fig. 1 shows the configuration of the proposed system. In PMSMs, the auxiliary windings which are used in the damping control (with the auxiliary inverter) are placed in the slots together with the main windings as shown in Fig. 2. The proposed system uses two different power rating inverters. The first one is the large power capacity inverter for the main windings to control the speed of the parallel connected PMSMs. The second one is a small power capacity inverter for the auxiliary windings to suppress the torque vibration. In term of the effectiveness of the proposed system, it is very important that the power capacity of the auxiliary inverter is enough small. In other words, the damping power for the PMSM is much smaller than that of the main drive power.

Fig. 3 shows the control block diagram of the proposed system. In the proposed system, the main inverter is applied with the V/f control and the auxiliary inverter is applied with the field-oriented control and the damping controls. Each of the auxiliary inverter can control the current in auxiliary windings of the PMSM in order to suppress the torque and speed vibration. Since the torque and
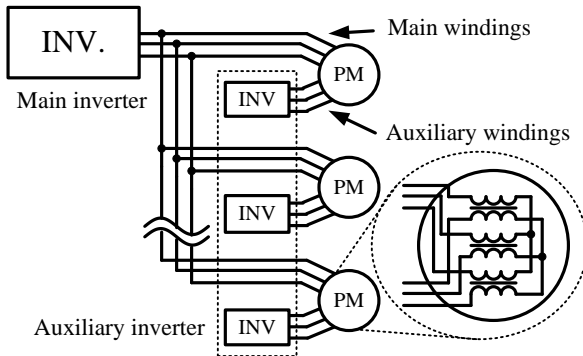
Fig. 1.Configuration of the proposed system. The proposed system uses two different power rating inverters, the large power capacity inverter to drive the motors and the small power capacity inverter to suppress the vibration.
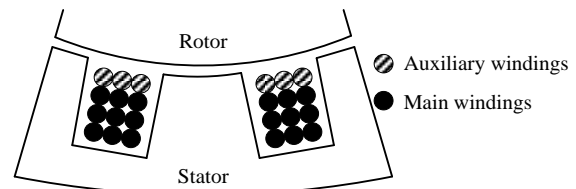
Fig. 2. Main windings and auxiliary windings. The number of the auxiliary winding is less than the numbers of the main windings.
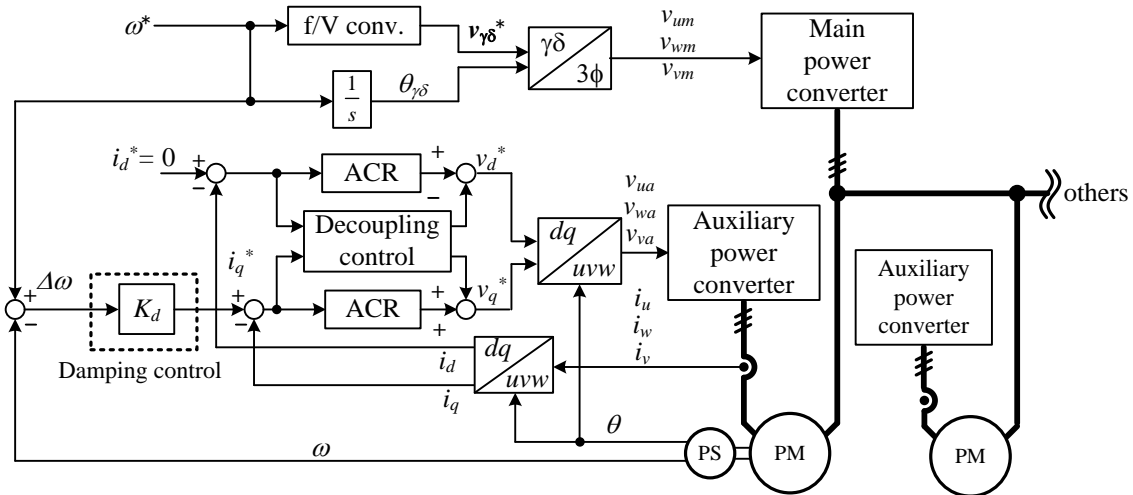
Fig. 3.Control block diagram of the proposed system. The V/f control is applied to the main inverter and the auxiliary inverters uses the field-oriented control for the damping control.

ω : Rotational speed
ω^*: Rotational speed command
v : Output voltage
e : Electro-motive force
δ : Load angle
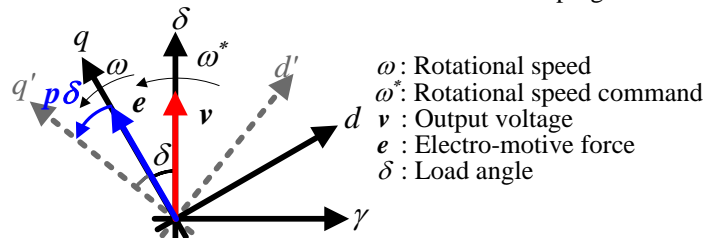
Fig.4. Relationship between the d-q reference frame and the estimated rotating γ–δ frame. The estimated rotating γ-δ frame lags by the load angle δ from the d-q reference frame.

speed vibrations are caused by the phase difference between the rotational coordinates of the inverter and of the PMSM, it can be suppressed by the damping control in the auxiliary inverter.

Fig. 4 shows the relationship between the d-q reference frame and the estimated rtating γ-δ frame in. a V/f control. In V/f control, the output voltage vector direction is defined as δ-axis, the axis which lags by π/2 rad from δ-axis can be defined as γ-axis. The lag of the load angle δ occurs between the d-q refrence frame and estimated rotating γ-δ frame as shonwn in Fig. 4. Therefore, the load angle δ and rotational speed ω_{re}, the speed command ω^* can be expressed as

$$p\delta = \omega_{re} - \omega^* \dots\dots\dots\dots\dots\dots\dots\dots\dots\dots\dots\dots\dots\dots\dots\dots\dots\dots\dots\dots\dots\dots\dots\dots\dots\dots\dots (1)$$

When the vibration of the speed is caused by the resonance between the inertia moment and the synchronous reactance, the load angle δ also is vibrating as shown (1). Then, notice that the changes of load angle $p\delta$ is the difference between the rotational speed and the speed command, in order to compensate the changes of load angle $p\delta$, the q-axis current command i_q^* is calculated from the damping controller as shown in Fig. 3. As a result, the vibration of the speed and torque caused by the resonance are suppressed by compensating the changes of the load angle with the current controlled by the field-oriented control and the damping control.

3. Stability analysis

The damping control has to suppress the speed and torque vibration caused the resonance between the inertia moment and the synchronous reactance. In this chapter, the stability of the proposed system with / without the damping control is clarified in a root locus. Besides, in the stability analysis, Surface Permanent Magnet Synchronous Motor is analyzed in order to simplify the stability analysis. However, in the case of Interior Permanent Magnet Synchronous Motor, the same stability can be also obtained.

Fig. 5 shows the experimental system to confirm the suppression effect with the damping control. The proposed system uses the PMSM placed the auxiliary windings in the slots together with the main (conventional) windings, and so the mutual magnetic interference occurs between the main and the auxiliary windings. Due to the above reason, the control for the auxiliary inverter becomes complicated. Therefore, the proposed system is validated using a model where two PMSMs are
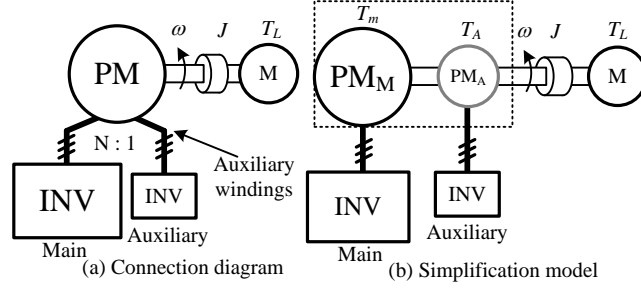
Figs. 5. Verification model of the PMSM in addition the auxiliary windings. Due to the mutual magnetic interference between the main and the auxiliary windings, this model is used to the verification.

connected in series via single shaft. Then, the rear end of the main PMSM is connected to the load machine. It means that the magnetic coupling was neglected in the simulation and the experiment.

Because it is impossible to control the current corresponding to the pole in the V/f control, the voltage equation of the motor that is connected to the main inverter is represented as the voltage equation in the estimated rotating γ-δ frame, which lags by the load angle δ from the d-q reference frame as shown in Fig. 4. On the other hand, the voltage equation of the motor that is connected to the auxiliary inverter is represented as the voltage equation in the d-q reference frame because the auxiliary inverter control is field-oriented control. Therefore, the voltage equation of the motor that is connected to the main inverter in the estimated rotating γ-δ frame is given by

$$\begin{bmatrix} v_{M\gamma} \\ v_{M\delta} \end{bmatrix} = \begin{bmatrix} R_M + pL_M & -\omega^* L_M \\ \omega^* L_M & R_M + pL_M \end{bmatrix} \begin{bmatrix} i_{M\gamma} \\ i_{M\delta} \end{bmatrix} + \omega_{re} \psi_{mM} \begin{bmatrix} \sin\delta \\ \cos\delta \end{bmatrix} \quad \text{.................................} (2)$$

On the other hand, the voltage equation of the motor that is connected to the auxiliary inverter in d-q reference frame can be given by

$$\begin{bmatrix} v_{Ad} \\ v_{Aq} \end{bmatrix} = \begin{bmatrix} R_A + pL_A & -\omega_{re} L_A \\ \omega_{re} L_A & R_A + pL_A \end{bmatrix} \begin{bmatrix} i_{Ad} \\ i_{Aq} \end{bmatrix} + \begin{bmatrix} 0 \\ \omega_{re} \psi_{mA} \end{bmatrix} \quad \text{.................................} (3)$$

Moreover, torque and speed equations can be given by

$$T = T_M - T_A = \frac{3}{2} P_f \psi_{mM} \left(i_\gamma \sin\delta + i_\delta \cos\delta \right) - \frac{3}{2} P_f \psi_{mA} i_q \quad \text{.................................} (4)$$

$$p\omega_{re} = \frac{P_f}{J} \left(T_M - T_A \right) \quad \text{.................................} (5)$$

where p is differential operator, R is armature resistance, L is synchronous reactance, P_f is pairs of the pole, Ψ_m is magnet flux linkage, and J is the inertia moment of motors, Suffix 'A' represents the parameter of the motor that is connected to the auxiliary inverter, 'M' represents the parameter of the motor that is connected to the main inverter.

The equations (2) and (3), (4) are non-linear so that these equations are linearized in the stationary neighborhood. The state equation after the linearization can be given by

$$p\mathbf{x} = \mathbf{A}\mathbf{x} + \mathbf{B}\mathbf{u} \quad \text{.................................} (6)$$

where $\mathbf{x} = \begin{bmatrix} \Delta i_{M\gamma} & \Delta i_{M\delta} & \Delta i_{Ad} & \Delta i_{Aq} & \Delta\omega_{re} & \Delta\delta \end{bmatrix}$, $\mathbf{u} = \begin{bmatrix} \Delta v_{M\gamma} & \Delta v_{M\delta} & \Delta v_{Ad} & \Delta v_{Aq} & \Delta\omega^* \end{bmatrix}$,

$$\mathbf{A} = \begin{bmatrix} -\dfrac{R_M}{L_M} & \omega_0 & 0 & 0 & -\dfrac{\psi_m}{L_M}\sin\delta_0 & -\dfrac{\omega_0\psi_m}{L_M}\cos\delta_0 \\[2mm] -\omega_0 & -\dfrac{R_M}{L_M} & 0 & 0 & -\dfrac{\psi_m}{L_M}\cos\delta_0 & \dfrac{\omega_0\psi_m}{L_M}\sin\delta_0 \\[2mm] 0 & 0 & -\dfrac{R}{L_A} & 0 & 0 & 0 \\[2mm] 0 & 0 & 0 & -\dfrac{R}{L_A} & 0 & 0 \\[2mm] \dfrac{3}{2}\dfrac{P_f^2\psi_m}{J}\sin\delta_0 & \dfrac{3}{2}\dfrac{P_f^2\psi_m}{J}\cos\delta_0 & 0 & \dfrac{3}{2}\dfrac{P_f^2\psi_m}{J} & 0 & \dfrac{3}{2}\dfrac{P_f^2\psi_m}{J}\left(i_\gamma\cos\delta_0 - i_\delta\sin\delta_0\right) \\[2mm] 0 & 0 & 0 & 0 & -1 & 0 \end{bmatrix},$$

$$\mathbf{B} = \begin{bmatrix} \dfrac{1}{L_M} & 0 & 0 & 0 & i_{M\delta0} \\ 0 & \dfrac{1}{L_M} & 0 & 0 & -i_{M\gamma0} \\ 0 & 0 & \dfrac{1}{L_A} & 0 & 0 \\ 0 & 0 & 0 & \dfrac{1}{L_A} & 0 \\ 0 & 0 & 0 & 0 & 0 \\ 0 & 0 & 0 & 0 & 1 \end{bmatrix}$$

The equation (6) shows the 6th degree of the state equation that is complicated to evaluate the stability. In order to simplify this equation, assuming that the mechanical time constant is larger than electrical time constant, then (6) can be approximated as the 2nd state equation, as follows:

$$\begin{bmatrix} p\Delta\omega_{re} \\ p\Delta\delta \end{bmatrix} = \begin{bmatrix} 0 & \dfrac{3}{2}\dfrac{P_f^2\psi_{mM}}{J}\left(\dfrac{\psi_{mM}}{L_M}+i_{M\gamma0}\cos\delta_0-i_{M\delta0}\sin\delta_0\right) \\ -1 & 0 \end{bmatrix}\begin{bmatrix} \Delta\omega_{re} \\ \Delta\delta \end{bmatrix}$$

$$+\begin{bmatrix} \dfrac{3}{2}\dfrac{P_f^2\psi_m}{J}\dfrac{\sin\delta_0}{\omega_0 L_M} & -\dfrac{3}{2}\dfrac{P_f^2\psi_m}{J}\dfrac{1}{R_A} & -\dfrac{3}{2}\dfrac{P_f^2\psi_m}{J}\dfrac{\left((\omega_0 L_M+R_M)i_{M\delta0}\sin\delta_0+(\omega_0 L_M-R_M)i_{M\gamma0}\cos\delta_0\right)}{\omega_0^2 L_M} \\ 0 & 0 & 1 \end{bmatrix}\begin{bmatrix} \Delta v_\delta \\ \Delta v_q \\ \Delta\omega^* \end{bmatrix}$$

.... (7)

where suffix '0' is the operating point.

In addition, (7) assumes that the field oriented control is applied with the non-interference control
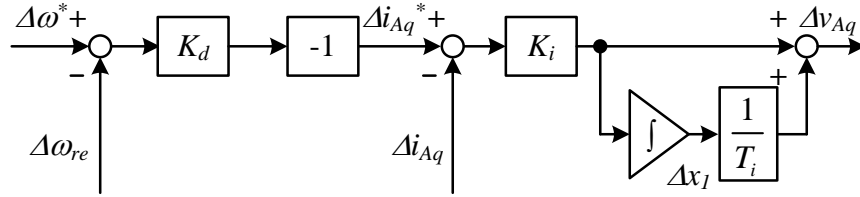
Fig. 6.State variable diagrams of the auxiliary inverter control. If the current control response is faster than the damping control response, the loop gain in the current control is 1. Therefore, the q-axis voltage command $\Delta v_{Aq}*$ can be given by (10).

and the γ-axis voltage command $\Delta v_{M\gamma}*$ of the main inverter is zero as shown in Fig. 4. Notice the state transition matrix A of (7), the characteristic equation can be solved as ωL is larger than R.

Fig. 6 shows the state variable diagrams of the auxiliary inverter control that is applying the damping control. Notice in Fig. 6, the q-axis voltage command of the auxiliary inverter and the input of the integrator in the damping control $p\Delta x_1$ are given by

$$\Delta v_{Aq} = -K_i K_d\left(\Delta\omega^*-\Delta\omega_{re}\right)-K_i\Delta i_{Aq}+\dfrac{1}{T_i}\Delta x_1 \quad\text{.. (8)}$$

$$p\Delta x_1 = -K_i K_d\left(\Delta\omega^*-\Delta\omega_{re}\right)-K_i\Delta i_{Aq} \quad\text{.. (9)}$$

However, in Fig. 6, the q-axis voltage command $\Delta v_{Aq}*$, assuming that the loop gain in the current control is 1 (assuming that the current control response is faster than the damping control response), can be given by

$$\Delta v_{Aq} = -K_d\left(\Delta\omega^*-\Delta\omega_{re}\right) \quad\text{...(10)}$$

$$p\Delta x_1 = 0 \quad\text{...(11)}$$

Moreover, in Fig. 3, the δ-axis voltage command $\Delta v_{M\delta}*$ of the main inverter is given by

$$\Delta v_{M\delta} = \psi_{mM}\Delta\omega^* \quad\text{..(12)}$$

Substituting the equation (10) and (12) into t (7) yields the state equation of

Table I: Verification condition

	PM$_1$&PM$_2$		PM$_1$&PM$_2$
Rated power [W]	800	Synchronous inductance $L_M \ L_A$ [mH]	3.78
Rated speed [min^{-1}]	2000	Armature resistance $R_M \ R_A$ [Ω]	0.425
Rated torque [Nm]	3.82	Electro-motive force constant $\psi_M \ \psi_A$ [Vs/rad]	0.233
Rated current [A]	8.2	Inertia momet $J_M \ J_A$ [kgm^2]	0.018
Number of pole pairs P_f	2	Rotational Speed in stationary state ω_0 [rad/s]	335
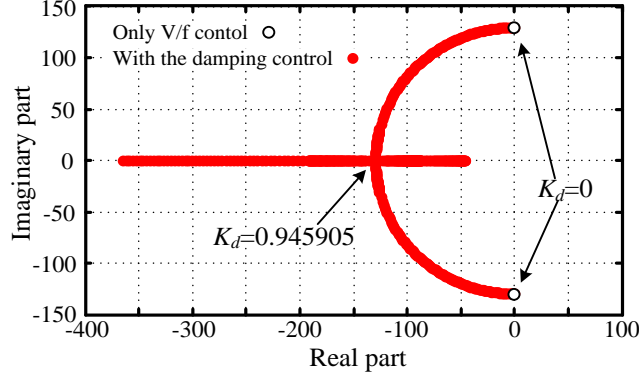
Fig.7. Root locus with the control structures in the proposed system. Table I shows the evaluated condition. When the damping control is not applying, it shows that the proposed system is unstable. By contrast, when the damping gain Kd increases, the poles move into left half plane.

$$\begin{bmatrix} p\Delta\omega_{re} \\ p\Delta\delta \end{bmatrix} = \begin{bmatrix} -\dfrac{3}{2}\dfrac{P_f^2\psi_{mM}}{J}K_d & \dfrac{3}{2}\dfrac{P_f^2\psi_{mM}}{J}\left(\dfrac{\psi_{mM}}{L_M}+i_{M\gamma0}\cos\delta_0-i_{M\delta0}\sin\delta_0\right) \\ -1 & 0 \end{bmatrix}\begin{bmatrix} \Delta\omega_{re} \\ \Delta\delta \end{bmatrix}$$
$$+\begin{bmatrix} \dfrac{3}{2}\dfrac{P_f^2\psi_{mM}}{J}\left(K_d+\dfrac{\psi_{mM}\sin\delta}{\omega_0 L_M}-\dfrac{(i_{\delta0}\sin\delta+i_{\gamma0}\cos\delta_0)}{\omega_0}\right) \\ 1 \end{bmatrix}\Delta\omega^* \quad\text{.........................(13)}$$

Notice the state transition matrix A of (13), assumed as $\delta_0 = 0$, $i_{M\gamma0} = 0$, $i_{M\delta0} = 0$, the characteristic equation can be solved as ωL is larger than R, as given by

$$s = -\frac{3}{2}\frac{P_f^2\psi_m}{2J}K_d \pm \sqrt{\frac{3}{2}}\frac{P_f\psi_m}{\sqrt{JL_M}}\sqrt{\left(\sqrt{\frac{3}{2}}P_f\frac{K_d}{2}\sqrt{\frac{L_M}{J}}\right)^2-1} \quad\text{...(14)}$$

As a result, Fig. 7 shows the transition of the pole placement (the root locus) when applying the damping control when the damping gain K_d is gradually changed. At the damping gain $K_d = 0$, the poles are placed on the imaginary axis. In other words, when the damping control is not applying, it shows that the proposed system is unstable. By contrast, when the damping gain K_d increases, the poles move into left half plane. Therefore, PMSM can be driven stably in the proposed system by applying the damping control.

4. Simulation for parallel drive operation

In previous chapter, the stability of the proposed system is discussed with / without the damping control. In this chapter,

Fig. 11 shows the simulation models that are used to verify the operation of two sets of parallel connected PMSM. As mentioned above, in order to neglect the magnetic coupling in the simulation, the model where two PMSMs are connected in series via single shaft is used in the simulation.

Fig. 12 shows the simulation results when two sets of parallel connected PMSMs are driven by the proposed system with the damping control as shown in Fig. 7. Smooth acceleration progresses are confirmed in the two set of parallel connected PMSMs. Besides, when the rated motor speed, load step
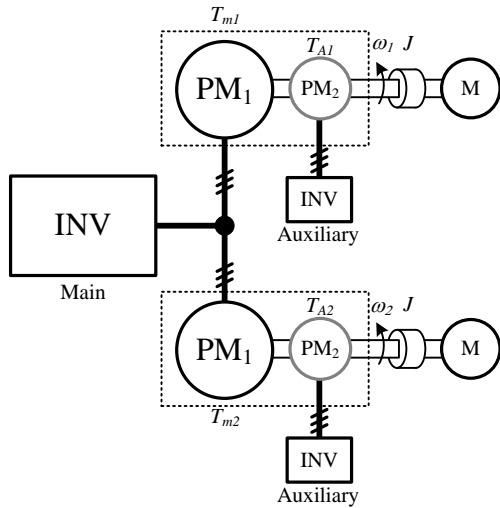
Fig. 11. Simulation model for parallel connected dual motor drive. In order to neglect the magnetic coupling in the simulation and the experiment, two parallel drive of the proposed system is validated using Fig. 7 as shown in Fig. 5(b).
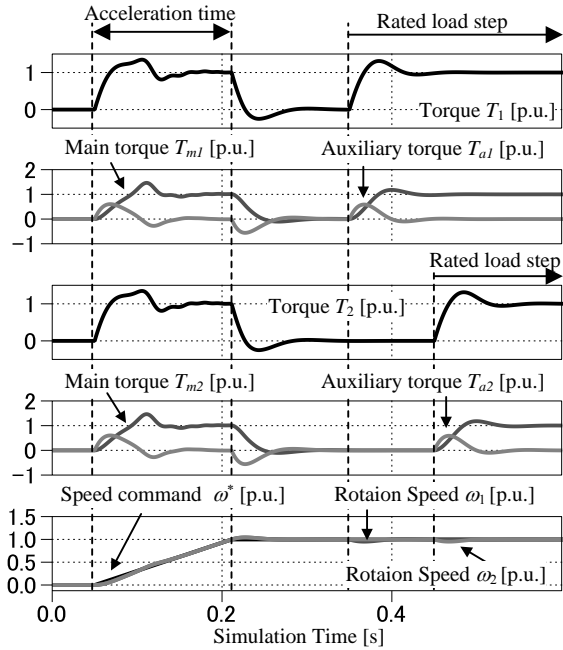
Fig. 12. Simulation results for parallel operation with damping control based on the field-oriented control.

applies to PMSM1 at 0.38s, and later also applies to PMSM2 at 0.42s, the operation of the two auxiliary inverters can be observed from the output power. The maximum output power of the auxiliary inverter is approximately 0.25 p.u. of the rated power of the main inverter. Although the power capacity of main inverter increases with the increase of parallel units, the power capacity of auxiliary inverter does not change according to the numbers of parallel units.

5. Experimental results to confirm the suppression effect with the damping control

In this chapter, in order to confirm the effectiveness of the damping control, the experiments are conducted with a motor –generator set.

Figs. 8 show the relationship between the simulation model and the motor-generator set in this paper. Since the model is constructed from two PMSMs that are connected in series via single shaft as shown in Fig. 4 (b), if the load machine is removed as shown in Fig. 8 (a), then it is equal to the motor- generator set as shown in Fig. 8 (b).

Fig. 9 shows the experimental configuration to confirm the effectiveness of the damping control in the proposed system. As mentioned above, the effectiveness of the proposed system can be verified with the motor-generator set as shown Fig. 9. Therefore, in order to confirm the effectiveness of the proposed damping control, the experiment is performed with the M-G set as shown in Fig. 9.

Figs. 10 show the experimental results that illustrate the motor speed vibration when the proposed

(a) Simplification model   (b) Motor – Generator set
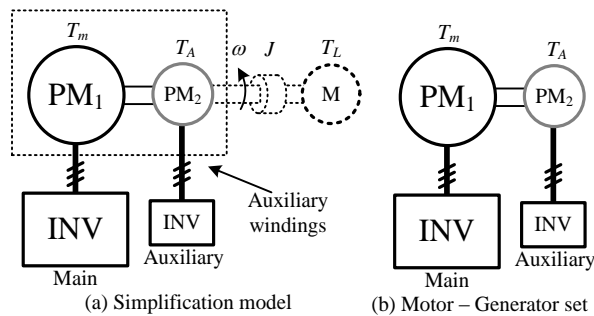
Figs. 8. Simulation model and motor-generator set. If the load machine is removed from (a), then it is equal to the motor-generator set as shown (b).

	Motor	Load
Rated power	: 1.5 kW	750 W
Rated speed	:1800 r/min	1800 r/min
Rated current	: 6.1 A	3 A
Number of pole	: 3	3
d-axis inductance	: 11.5mH	15.2mH
q-axis inductance	: 23mH	33.2mH
Armature resistance	: 0.522Ω	1.975Ω
Flux-linkage	: 0.368Wb	0.338Wb
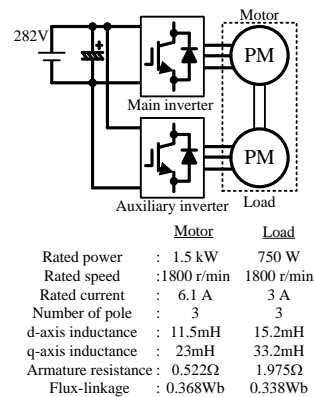
Fig. 9. Experimental configuration and condition
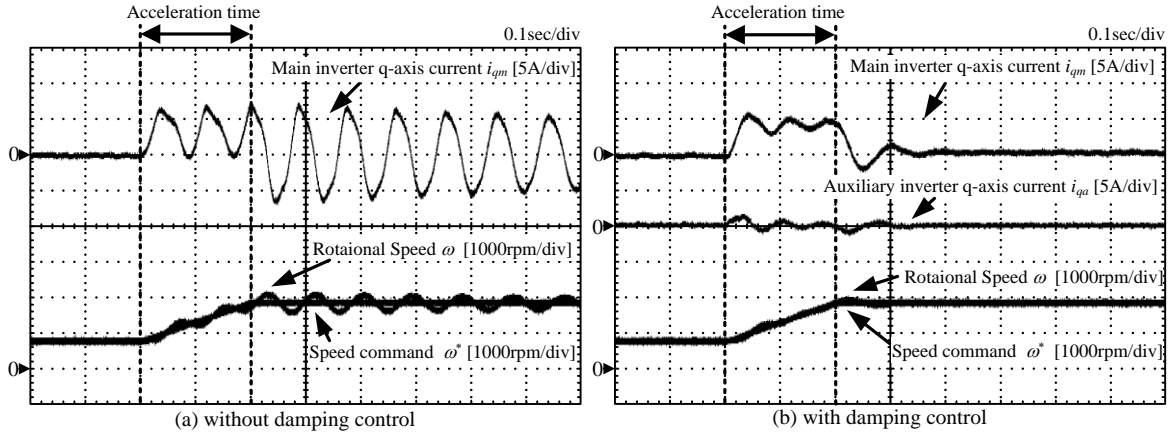
Figures 10. Acceleration test without/with damping control in motor-generator set. (a) After the acceleration, the 400 r/min - speed vibration is maintained. (b) The speed vibration is reduced from 400 r/min to nearly 0 r/min in compared with (a) by applying the damping control.

system is applied (a) without the damping control and (b) with the damping control in an acceleration test. In this experiment, it is difficult to measure the torque response directly. Therefore, the speed vibration is evaluated instead of the torque response. In Fig. 10 (a), the proposed system is implemented without damping control. The speed vibration can be noticed during the acceleration. After the acceleration, a 400 r/min of speed vibration and the 10 Ap-p of current vibration in q-axis of the main inverter are maintained. On the other hand, Fig. 10 (b) demonstrates the experimental results, where the proposed system is implemented with the damping control. The effectiveness of the auxiliary inverter can be noticed from the result that the speed vibration is reduced from 400 r/min to nearly 0 r/min in compared with Fig. 10 (a). The 10 Ap-p of current vibration in the q-axis of the main inverter as shown in Fig. 10 (a) can be suppressed as well.

6. Consideration about the relationship between the damping gain and the output power of the auxiliary inverter

In the previous section, it is confirmed that the PMSM can be driven in the proposed system in the experiment. However, if the damping gain K_d increases to obtain the larger suppression effect, the output power of the auxiliary inverter becomes larger. Thus, in this section, the relationship between the damping gain K_d and the output power of the auxiliary inverter is clarified.

The speed command $\Delta\omega^*$ to the rotational speed $\Delta\omega_{re}$ transfer function is given by

$$\frac{\Delta\omega_{re}}{\Delta\omega^*} = \frac{\frac{3}{2}\frac{P_f^2\psi_{mM}}{J}\left(\frac{\psi_{mM}}{L_M} + \left(i_{M\gamma}\cos\delta_0 - i_{M\delta}\sin\delta_0\right) - s\left(K_d + \frac{\left(i_{M\gamma}\cos\delta_0 + i_{M\delta}\sin\delta_0\right)}{\omega_0} - \frac{\psi_{mM}}{\omega_0 L_M}\sin\delta_0\right)\right)}{s^2 + \frac{3}{2}\frac{P_f^2\psi_{mM}}{J}K_d s + \frac{3}{2}\frac{P_f^2\psi_{mM}}{J}\left(\frac{\psi_{mM}}{L_M} + \left(i_{M\gamma}\cos\delta_0 - i_{M\delta}\sin\delta_0\right)\right)}$$

.... (15)

The time response of the rotational speed is derived from the inverse Laplace transform of the ramp response of (15). In this section, in order to simplify (15), the equation (15) is assumed as $\delta_0 = 0$, $i_{M\gamma 0} = 0$, $i_{M\delta 0} = 0$. Moreover, the overshoot of the rotational speed can be derived from this time response, as given by

$$\Delta\omega_{re\_Overshoot} = \frac{\alpha\sin\left(\omega_n t_{peak}\sqrt{1-\zeta^2}\right)}{\omega_n\sqrt{1-\zeta^2}\exp\left(\zeta\omega_n t_{peak}\right)}$$ .... (16)

$$t_{peak} = \frac{1}{2}\frac{\log\left(2\zeta^2 - 1 + 2\zeta\sqrt{\zeta^2-1}\right)}{\omega_n\sqrt{\zeta^2-1}}$$ .... (17)

$$\zeta = \sqrt{\frac{3}{2}}\frac{P_f K_d}{2}\sqrt{\frac{L_M}{J}}$$ .... (18)

where α is acceleration [rad/s^2].

The overshoot of the rotational speed can be calculated by using (16).

If the electrical and mechanical losses are neglected, the output power of the auxiliary inverter, depends on the mechanical output of the motor. In other words, the transfer function of the output power for the auxiliary inverter is derived from the mechanical output transfer function of the motor. However, the mechanical output is nonlinear because the mechanical output is the product of two variables, the rotational speed and the torque. Due to this reason, the output power transfer function of the auxiliary inverter is derived after the mechanical output is linearized. The speed command $\Delta\omega^*$ to the output power of the auxiliary inverter transfer function is given by

$$\frac{\Delta P_A}{\Delta \omega^*} = \frac{s \frac{3}{2}\omega_0 K_d \psi_{mA}\left(s + \frac{3}{2}\frac{P_f^2 \psi_{mM}}{J\omega_0}\left(\left(i_{M\gamma}\cos\delta_0 + i_{M\delta}\sin\delta_0\right) - \frac{\psi_{mM}}{L_M}\sin\delta_0\right)\right)}{s^2 + \frac{3}{2}\frac{P_f^2\psi_{mM}}{J}K_d s + \frac{3}{2}\frac{P_f^2\psi_{mM}}{J}\left(\frac{\psi_{mM}}{L_M} + \left(i_{M\gamma}\cos\delta_0 - i_{M\delta}\sin\delta_0\right)\right)} \quad \text{......................(19)}$$

The time response of the output power of the auxiliary inverter during the acceleration is also derived from the inverse Laplace transform of the ramp response of (19). In this section, in order to simplify the equation (19), the equation (19) is assumed as $\delta_0 = 0$, $i_{M\gamma 0} = 0$, $i_{M\delta 0} = 0$. Moreover, the maximum output power of the auxiliary inverter can be derived from this time response, as given by

$$\Delta P_{aPeak} = \frac{\frac{3}{2}P_f \psi_{mA} K_d \omega_0 \alpha \sin\left(\omega_n \sqrt{1-\zeta^2}\,t_{peak}\right)}{\omega_n \sqrt{1-\zeta^2}\,\exp\left(\zeta\omega_n t_{peak}\right)} \quad \text{...(20)}$$

The maximum output power of the auxiliary inverter can be calculated by using (20).

Figs. 13 (a) and (b) show the relationship among the damping gain K_d, the maximum output power of the auxiliary inverter during the acceleration and the overshoot of the rotational speed when the PMSM is accelerated during one, twice, four times of the rated acceleration time on the condition as shown in Table 1. The damping gain is standardized by the damping factor ζ as given by (18). The output power of the auxiliary inverter rises with the increase of the damping factor. On the other hand, the overshoot of the rotational speed decreases with the increase of the damping factor, as shown in Fig. 13(b). In other words, the higher suppression effect is obtained by increasing the damping gain. However, from the point of the view of the power capacity of the auxiliary inverter, it needs to decrease the output power of the auxiliary inverter. In Fig. 13, if the output power is reduced to 0.1 p.u., the output power of the auxiliary inverter can be suppressed, under condition that the damping factor is smaller than 0.1p.u by adjusting the damping gain. On the other hand, if the proposed system is applied to the constant speed drive system, decreasing the power capacity of the auxiliary inverter can be expected so that the maximum output power of the auxiliary inverter depends on the acceleration time as shown Fig. 13(a). The results show that, if the application that is required a slow response is applied to the proposed system such as fan applications, the power capacity of the auxiliary inverter can be designed to nearly 10% of the main inverter.
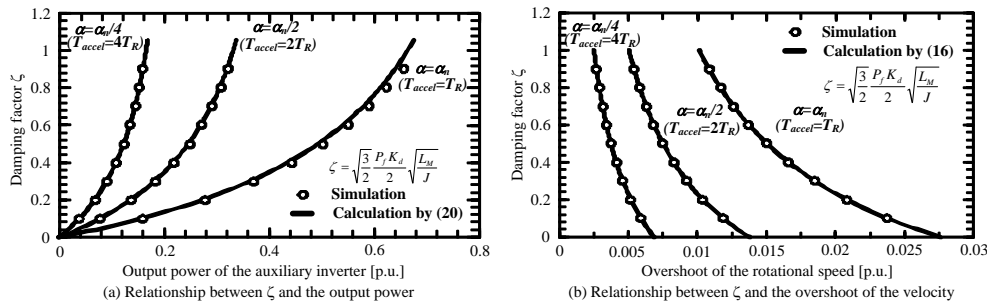
Figs. 13. Relationship between the damping factor ζ and the output power of the auxiliary inverter. Table I show also the evaluated condition. α_n is the rated acceleration [rad/s^2]. T_R is the rated acceleration time. T_{accel} is the real acceleration time. The higher suppression effect is obtained in exchange for the increase of the output power of the auxiliary inverter by increasing the damping gain However, if the application that is required a slow response is applied to the proposed system, the power capacity of the auxiliary inverter can be designed to nearly 10% of the main inverter.

7. Conclusion

This paper discusses a control technique to dive multiple numbers of parallel connected PMSMs. The features of the proposed system are following;

- The proposed system is composed by two different inverters, which are the main inverter for speed control in parallel and the small power capacity auxiliary inverter to suppress the torque and speed vibration.

- In addition to the conventional windings (main windings) for the motor drive, each of the PMSM is added with auxiliary windings to suppress the torque vibration.

- The power capacity of the auxiliary inverter is small because the auxiliary inverter is operated when the torque vibration needs to be suppressed.

From the stability analysis of the root locus, it was clarified that the PMSM can be stabilized by applying the damping control in the proposed system. The experimental results demonstrated that the proposed system can reduce the speed vibration from 400 r/min to nearly 0 r/min in spite of small q-axis current by suppressing the torque vibration by applying damping control to the auxiliary inverter. For the experimental results, it was confirmed that the proposed system can be driven stably.

In addition, the relationship between the damping gain and the output power of the auxiliary inverter is clarified. The results show that, if the application that is required a slow response is applied to the proposed system such as fan applications, the power capacity of the auxiliary inverter can be designed to nearly 10% of the main inverter.

In the future work, the internal structure of the auxiliary windings in PMSM of the proposed system will be considered. Secondly, driving several units of motor-generator in parallel with the proposed system drives will be considered.

References

[1] P. M.Kelecy and R. D. Lorenz, "Control methodology for single inverter, parallel connected dual induction motor drives for electric vehicles," in Proc. IEEE PESC'94, pp.987–991 (1994)

[2] Matsuse, K. ; Kouno, Y. ; Kawai, H. ; Yokomizo, S.: "A speed-sensorless vector control method of parallel-connected dual induction motor fed by a single inverter", IEEE Trans. Industry Applications., Vol.38, pp.1566-1571 (2002)

[3] Ibrahim, Z.; Lazi, J.M.; Sulaiman, M.: "Independent speed sensorless control of dual parallel PMSM based on Five-Leg Inverter ", Systems, Signals and Devices, 9th International Multi-Conference, pp.1-6 (2012)

[4] Nozawa, Y, Oka, K., Omata, R, Matsuse, K.: "Performance for Position Control of Two Permanent Magnet Synchronous Motors with the Five-Leg Inverter.", IECON'06, pp.1182-1187 (2006)

[5] S. Mohammad D. Dehnavi, M. Mohamadian, A. Yazdian, F. Ashrafzadeh: "Space Vectors Modulation for Nine-Switch Converters", IEEE Trans. Power Electronics., Vol.25, pp.1488-1496 (2010)

[6] Shibata, M., Hoshi, N.: "Novel inverter topologies for two-wheel drive electric vehicles with two permanent magnet synchronous motors", 12th European Conference on Power Electronics and Applications (2007)

[7] Chiasson, J., Danbing Seto, Fanping Sun, Stankovic, A., Bortoff, S.: "Independent Control of two PM motors using a single inverter: Application to Elevator Doors.", American Control Conference, Vol.4, pp.3093-3098 (2002)

[8] D. Bidart, M. Pietrzak-David, P. Maussion, M. Fadel: "Mono inverter dual parallel PMSM - Structure and Control strategy", IECON'08, pp.268-273 (2008)

[9] Bidart, D., Pietrzak-David, M., Maussion, P., Fadel, M., "Mono inverter multi-parallel permanent magnet synchronous motor: structure and control strategy", Electric Power Applications, IET, Vol.5, pp.288-294 (2011)

[10] J, Itoh, N, Nomura, H, Ohsawa: "A Comparison between V/f Control and Position-Sensorless Vector Control for the Permanent Magnet Synchronous Motor", Power Conversion Conference, pp.1310 - 1315 (2002)

[11] H. Plesko, J. Biela, J. Luomi, J. W. Kolar: "Novel Concepts for Integrating the Electric Drive and Auxiliary DC–DC Converter for Hybrid Vehicles", IEEE Trans. Power Electronics., Vol.23, No.6, pp.3025-3034 (2008)